Copy No.
RM No. A7L05

~~RESTRICTED~~






# RESEARCH MEMORANDUM

## AN INVESTIGATION OF THE DOWNWASH AND WAKE BEHIND LARGE-SCALE SWEPT AND UNSWEPT WINGS

By William H. Tolhurst, Jr.

Ames Aeronautical Laboratory
Moffett Field, Calif.



~~RESTRICTED DOCUMENT~~



NATIONAL ADVISORY COMMITTEE
FOR AERONAUTICS

WASHINGTON
February 2, 1948

~~RESTRICTED~~

NACA RM No. A7L05 [redacted]

NATIONAL ADVISORY COMMITTEE FOR AERONAUTICS

RESEARCH MEMORANDUM

# AN INVESTIGATION OF THE DOWNWASH AND WAKE BEHIND LARGE-SCALE SWEPT AND UNSWEPT WINGS

By William H. Tolhurst, Jr.

## SUMMARY

A wind-tunnel investigation has been conducted to determine, at large scale, the downwash angles, dynamic pressure loss, and wake width behind wings having sweep angles of $\pm 45^\circ$, $\pm 30^\circ$, and $0^\circ$. Data were obtained in a vertical transverse plane located at the probable tail position behind the wings for a region from the plane of symmetry to 0.7 semispan.

The results of this investigation indicate that the spanwise distribution of downwash was affected by sweep in a manner similar to span loading, increased toward the root by sweepforward and toward the tip by sweepback. After the first appearance of stall the downwash near the root of the swept-forward wing decreased markedly, probably as a result of loss of lift, while the downwash near the root of the swept-back wing increased, probably as a result of inboard movement of the tip vortices.

Sweep in the wing plan form modified the spanwise variation of wake thickness producing a thick wake near the root of swept-forward wings and near the tip of swept-back wings. At moderate to high angles of attack, sweep tends to keep the wake high.

## INTRODUCTION

Two of the most important factors affecting the design of a horizontal tail for an airplane are the downwash and wake of the wing at the tail. Extensive research has been conducted to determine the downwash angles and wake of unswept wings having various plan forms. In the case of swept wings, however, insufficient data regarding the downwash field and the wake have yet been obtained to enable analysis of the effect of wing sweep on tail-plane design.

[redacted]

In order to add to the knowledge of the downwash and wake characteristics of swept wings, a limited survey has been made of the downwash and wake behind wings having angles of sweep of 0, $\pm 30^\circ$, and $\pm 45^\circ$. These data were obtained during the investigation reported in reference 1, and the results are reported herein.

## SYMBOLS

| | |
|---|---|
| $C_L$ | lift coefficient (lift/qS) |
| $C_{L_\alpha}$ | rate of change of lift coefficient with angle of attack |
| $\epsilon$ | downwash angle, measured relative to the wind axes, degrees |
| $\epsilon_{max}$ | maximum downwash angle, degrees |
| $d\epsilon/d\alpha$ | rate of change of downwash angle with angle of attack |
| $d\epsilon_{max}/d\alpha$ | rate of change of maximum downwash angle with angle of attack |
| $\alpha$ | angle of attack, degrees |
| q | free-stream dynamic pressure, pounds per square foot |
| $q_T$ | dynamic pressure in the wake, pounds per square foot |
| $\Lambda$ | angle of sweep of quarter-chord line, degrees Sweepback is positive and sweepforward is negative. |
| A | aspect ratio ($b^2/S$) |
| b | wing span measured perpendicularly to plane of symmetry, feet |
| S | wing area, square feet |
| M.A.C. | mean aerodynamic chord, feet $\frac{2}{S}\int_0^{b/2} c^2 dy$ |
| X | longitudinal distance from a point at 0.25 M.A.C. to survey plane |
| Y | horizontal distance, perpendicular to plane of symmetry, semispan |

Z vertical distance above the extended chord plane, measured in a plane normal to the X-axis, semispan

## DESCRIPTION OF APPARATUS AND METHOD

Wing panels of each model were taken from a production airplane, having an NACA 0015 airfoil section at the root and an NACA 23009 airfoil section at the tip. The sweep angles of $\pm 45^\circ$, $\pm 30^\circ$, and $0^\circ$, measured from the quarter-chord line, were obtained by interchangeable center sections as described in reference 1. A sketch showing the geometric characteristics of each of the wings is presented in figure 1. Construction difficulties prevented the possibility of maintaining a consistent variation of either taper ratio or aspect ratio. The chord plane was maintained at $0^\circ$ dihedral throughout all configurations.

The wings were mounted in the Ames 40- by 80-foot wind tunnel on the three-strut support system. The survey rake consisting of six tubes of the combined pitch, yaw, and dynamic pressure type was mounted on a strut which allowed both vertical and horizontal movement of the rake. The strut was located to survey in a plane perpendicular to the X-axis approximately 2.8 M.A.C. behind a point at 0.25 M.A.C. of each of the wings. A photograph of the general test arrangement is shown in figure 2. Figure 3 shows the relation of the wings to the survey equipment.

For each of the wings, data were obtained at five spanwise stations for three angles of attack and at one spanwise station for an angle-of-attack range. The test was conducted at a dynamic pressure of approximately 20 pounds per square foot which resulted in Reynolds numbers, based on the M.A.C., ranging from 5,500,000 for the unswept wing to 9,100,000 for the $45^\circ$ swept-forward wing.

The angle of attack, downwash angle, and wake location have been corrected for air-stream inclination, tunnel-wall effect, and tare effect of the supporting boom and struts. It was found that the average tunnel-wall corrections with sweep were approximately the same as without sweep; therefore, the corrections for the unswept wing were used.

## RESULTS

Figure 4 presents contour maps showing lines of constant downwash angle in relation to vertical distance from the extended chord

plane of the wing. The change of maximum downwash angle with angle of attack is shown in figure 5 at one spanwise station for each of the wings. Curves from reference 1 showing the variation of lift coefficient with angle of attack for each of the five wings are presented in figure 6 in order to allow the downwash angle to be related to lift coefficient as well as angle of attack. The wake data are presented in figure 7 in terms of the maximum dynamic pressure loss in the wake and the vertical location of the wake limits in relation to the extended chord plane. (Limits of wake were taken as the point at which the dynamic pressure in the wake returned to 0.99 of free-stream dynamic pressure.) Due to the wide spacing of the rake tubes (fig. 3) it was not possible to define exactly the wake profile. The data as presented in figure 7 were taken from faired wake profiles and should show the qualitative effects of wing sweep on the wake.

## DISCUSSION

### Downwash

The general characteristics of the downwash field behind swept wings can be observed in the contour maps of figure 4. On swept-forward wings the maximum downwash occurs at the root. As the wing is swept back the point of maximum downwash moves outboard approaching the tip of the wing. This movement reflects the outward shift in loading due to sweepback as noted in reference 2.

The effect of downwash on the stability of an airplane having a horizontal tail can best be studied through the parameter $d\epsilon/d\alpha$. On unswept wings it can be demonstrated that $d\epsilon/d\alpha$ is very nearly proportional to $C_{L_\alpha}/A$. If, to a first approximation, this relationship holds for swept as well as unswept wings, then it might be expected that sweep would affect $d\epsilon/d\alpha$ only as sweep affects $C_{L_\alpha}$ (approximately $\cos \Lambda$ according to simple sweep theory).

For the wings considered in the present investigation the lift-curve slope and aspect ratio varied with sweep in such a manner as to keep the ratio $C_{L_\alpha}/A$ approximately constant; hence little change in the magnitude of $d\epsilon/d\alpha$ would be expected for the various wings. In figure 5 is shown the measured variation of maximum downwash angle with angle of attack for the various swept wings. Also shown is the estimated variation of maximum downwash angle with angle of attack based on the assumption that $d\epsilon_{max}/d\alpha$ is proportional to $C_{L_\alpha}/A$. If the slope of the linear portion of the experimental curve for the unswept wing is considered as the reference, the slopes of the corresponding portions of the curves of the swept-back wings

show little deviation from the predicted curves, while the curves of the swept-forward wings show slopes that are greater than predicted. The limited scope of this investigation prevents drawing of definite conclusions in this respect until further evidence can be gathered.

At high values of $C_L$ where stall begins on some sections of the wing, as indicated by tuft studies, the data of figure 5 indicate that the downwash angle continues to increase with angle of attack or remain nearly constant for the unswept and swept-back wings; whereas for the swept-forward wings the downwash angle shows a decrease. This may be explained by the fact that the unswept and swept-back wings stalled first at the tip causing the tip vortex core to move inboard exerting a stronger influence on the induced vertical velocity near the plane of symmetry. The swept-forward wing, on the other hand, stalled first at the center section and the induced velocity near the plane of symmetry is greatly reduced. For an airplane employing swept-forward wings and a tail this decrease in downwash should provide a large diving moment and thus aid in overcoming the tendency for longitudinal instability at high lift coefficients associated with most highly swept wings of high aspect ratio.

## Wake

The wake limits as shown in figure 7 indicate that the wing wake thickness increases toward the root of a swept-forward wing and toward the tip of a swept-back wing. This is probably the result of the spanwise flow in the boundary layer which tends to collect the low energy boundary-layer air at the root of the swept-forward wing and tip of the swept-back wing. In general, there is a gradual increase in wake width toward the root of swept-forward wings and toward the tip of swept-back wings. However, at high angles of attack, the wake of the 45° swept-forward wing shows a very rapid increase in width inboard of the 0.40 b/2 station; that is, at the 0.30 b/2 station the wake is 0.77 b/2 thick with indications of a greater increase further inboard. (The survey rake could not be raised high enough to cover the upper wake limit at the 0.185 b/2 station.) Similar results were reported in reference 3 for a 35° swept-forward wing. Observations of flow over the 45° swept-forward wing reported herein and other swept-forward wings indicate that this extreme wake thickness is probably the result of flow separation near the leading edge of the wing. Hence it is possible that a leading-edge modification such as a drooped nose, leading-edge flap, or a slot would succeed in reducing the wake width to more normal values. It might be presumed that a somewhat

similar pattern would have been found near the tip of the swept-back wings had the surveys been extended to the tip.

As in the case of unswept wings it appears that tail height through its control over $q_T/q$ experienced by the tail will also be important on swept wing designs. However, in contrast to most unswept wing designs in which it has been generally beneficial to keep the tail plane high and above the wake, it appears from these results that for swept wing designs, the rapid vertical spread of the wake (fig. 7) would dictate low tail plane positions. In the low position, the tail could be moving out of the wake as the angle of attack is increased, which would increase the stability. And further, at high angles of attack where a high degree of control is required, the tail would be operating out of the wake. Attention, however, must be given to requirements of ground clearance which could restrict tail heights to those in the wing chord plane or higher. Choice of a position in the wing chord plane may also be eliminated due to possible adverse effects of the tail lying in the wing wake at high speeds. Thus it may be impossible to take advantage of the potentially good low-speed stability and control characteristics associated with low tail positions.

## CONCLUDING REMARKS

Although the limited scope of this investigation prevents drawing of definite conclusions, certain trends of the effects of sweep on the downwash and wake behind wings are indicated. The effect of sweep on the spanwise distribution of downwash reflects the effects of sweep on the span loading; that is, sweepforward increases the downwash near the root while sweepback increases the downwash near the tip. With the first appearance of stall, the downwash at the root decreases for swept-forward wings as a result of a loss of lift over the wing root and increases on swept-back wings as a result of the inboard movement of the tip vortices.

Sweep increases the spanwise variation of wake thickness, the wake being generally thickest toward the root of swept-forward wing and the tip of swept-back wings. For moderate to high angles of attack increasing sweep tends to keep the wake high with respect to the extended chord plane of the wing.

Ames Aeronautical Laboratory,
National Advisory Committee for Aeronautics,
Moffett Field, Calif.

## REFERENCES

1. McCormack, Gerald M., and Stevens, Victor I., Jr.: An Investigation of Low-Speed Stability and Control Characteristics of Swept-Forward and Swept-Back Wings in the Ames 40- by 80-Foot Wind Tunnel. NACA RRM No. A6K15, 1947.

2. Van Dorn, Nicholas H., and DeYoung, John: A Comparison of Three Theoretical Methods of Calculating Span Load Distribution on Swept Wings. NACA RRM No. A7C31, 1947.

3. Luetgebrune, H.: Nachlauf- und Widerstandsunterschungen an Gepfeilten und Ungepfeilten Tragflügeln. Deutsche Luftfahrtforschung Forschungsbericht. Nr. 1672, Sept. 20, 1942.

NOTES

1. SWEEP ANGLES GIVEN ARE REFERRED TO QUARTER CHORD LINE OF AIRFOIL SECTIONS.
2. FORE & AFT LOCATION OF ROOT CHORD IS REFERRED TO .25 MAC.

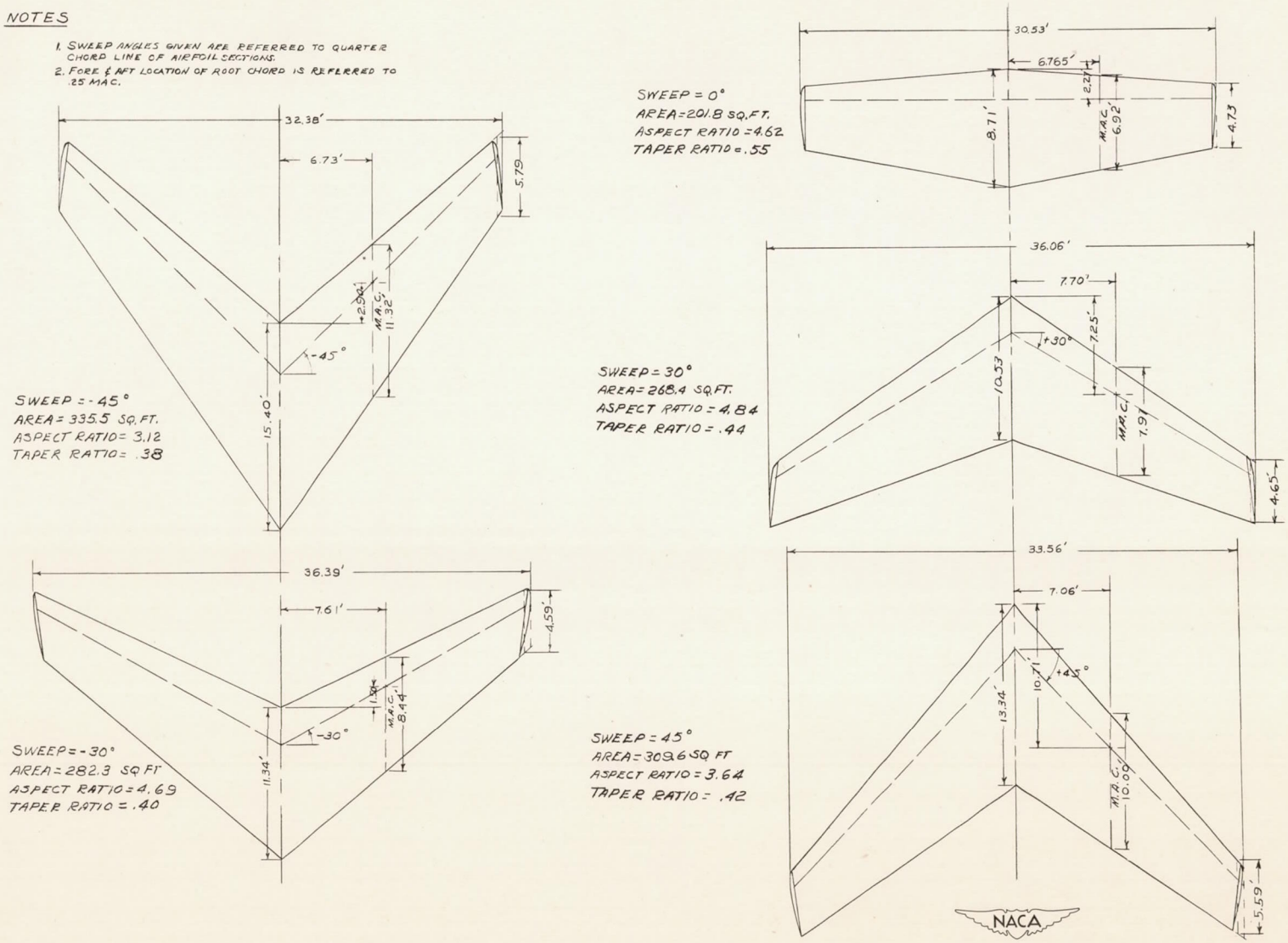


FIGURE 1. — GEOMETRIC CHARACTERISTICS OF THE WINGS

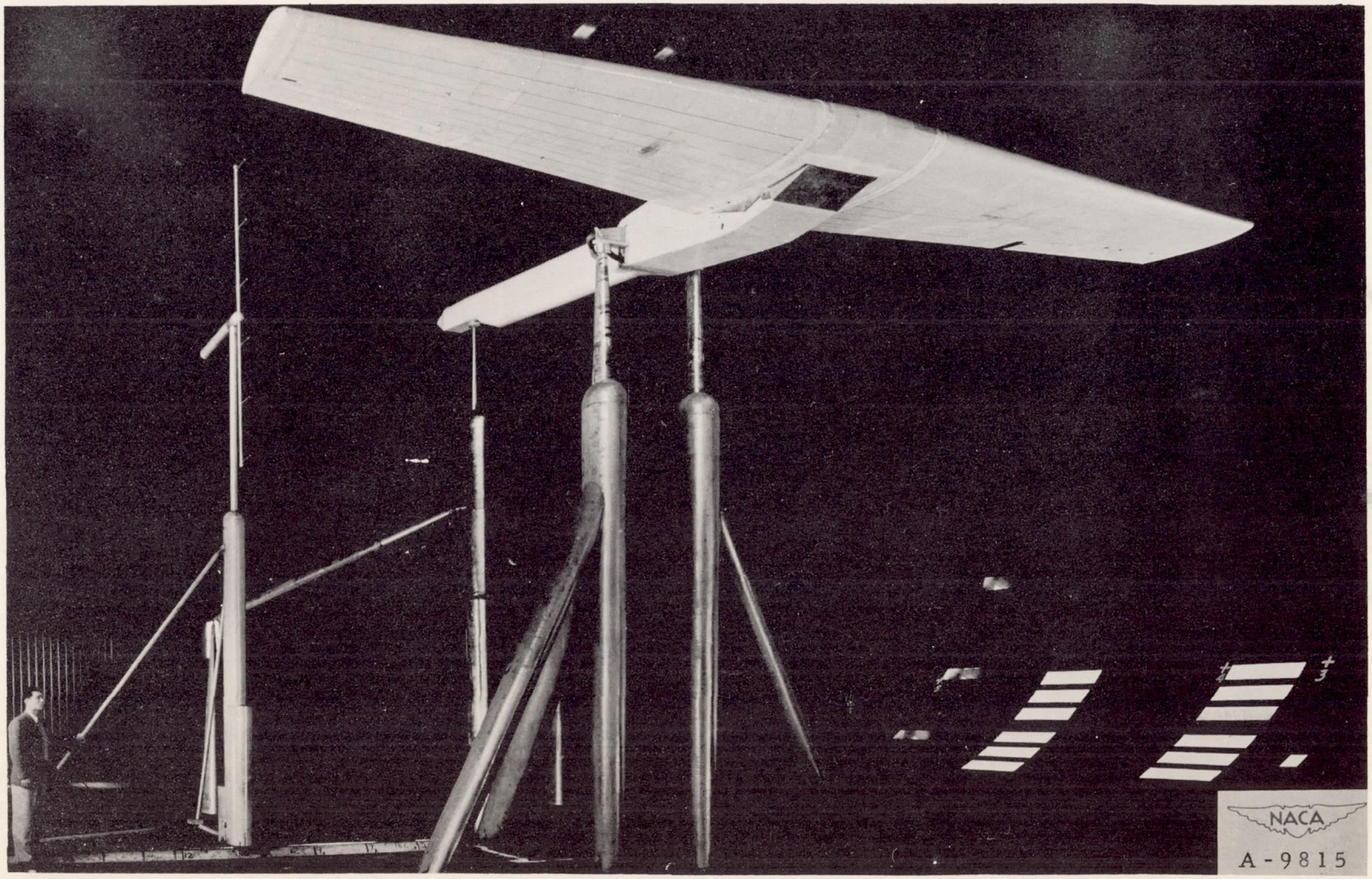


Figure 2.- The unswept wing mounted in the Ames 40- by 80-foot wind tunnel for downwash and wake surveys.

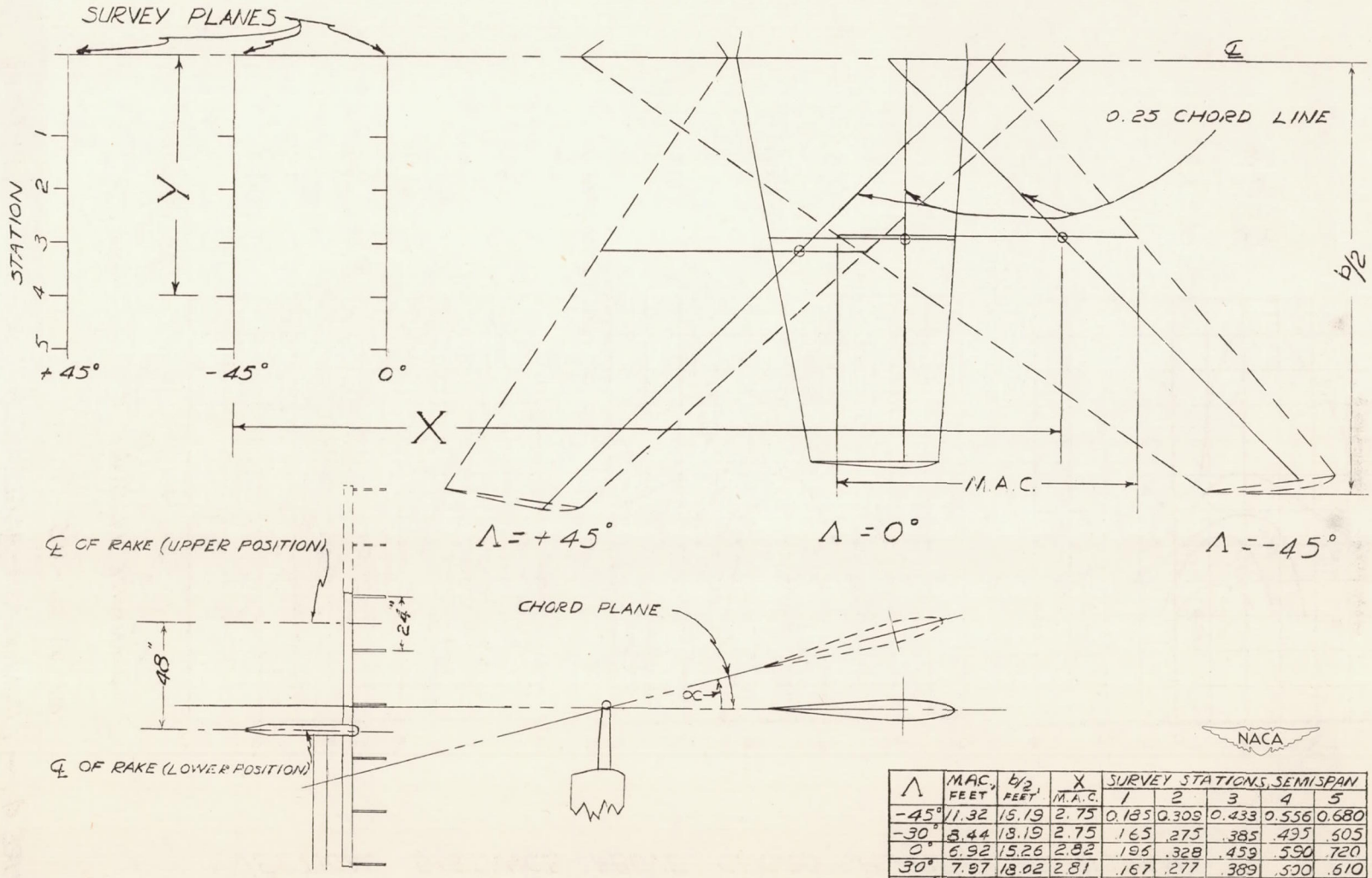


| Λ | M.A.C., FEET | b/2, FEET | X / M.A.C. | SURVEY STATIONS, SEMISPAN 1 | 2 | 3 | 4 | 5 |
|---|---|---|---|---|---|---|---|---|
| -45° | 11.32 | 15.19 | 2.75 | 0.185 | 0.309 | 0.433 | 0.556 | 0.680 |
| -30° | 8.44 | 18.19 | 2.75 | .165 | .275 | .385 | .495 | .505 |
| 0° | 6.92 | 15.26 | 2.82 | .196 | .328 | .459 | .590 | .720 |
| 30° | 7.97 | 18.02 | 2.81 | .167 | .277 | .389 | .500 | .610 |
| 45° | 9.99 | 16.78 | 2.75 | .179 | .298 | .417 | .536 | .656 |

FIGURE 3.— GEOMETRICAL ARRANGEMENT OF SURVEY APPARATUS.

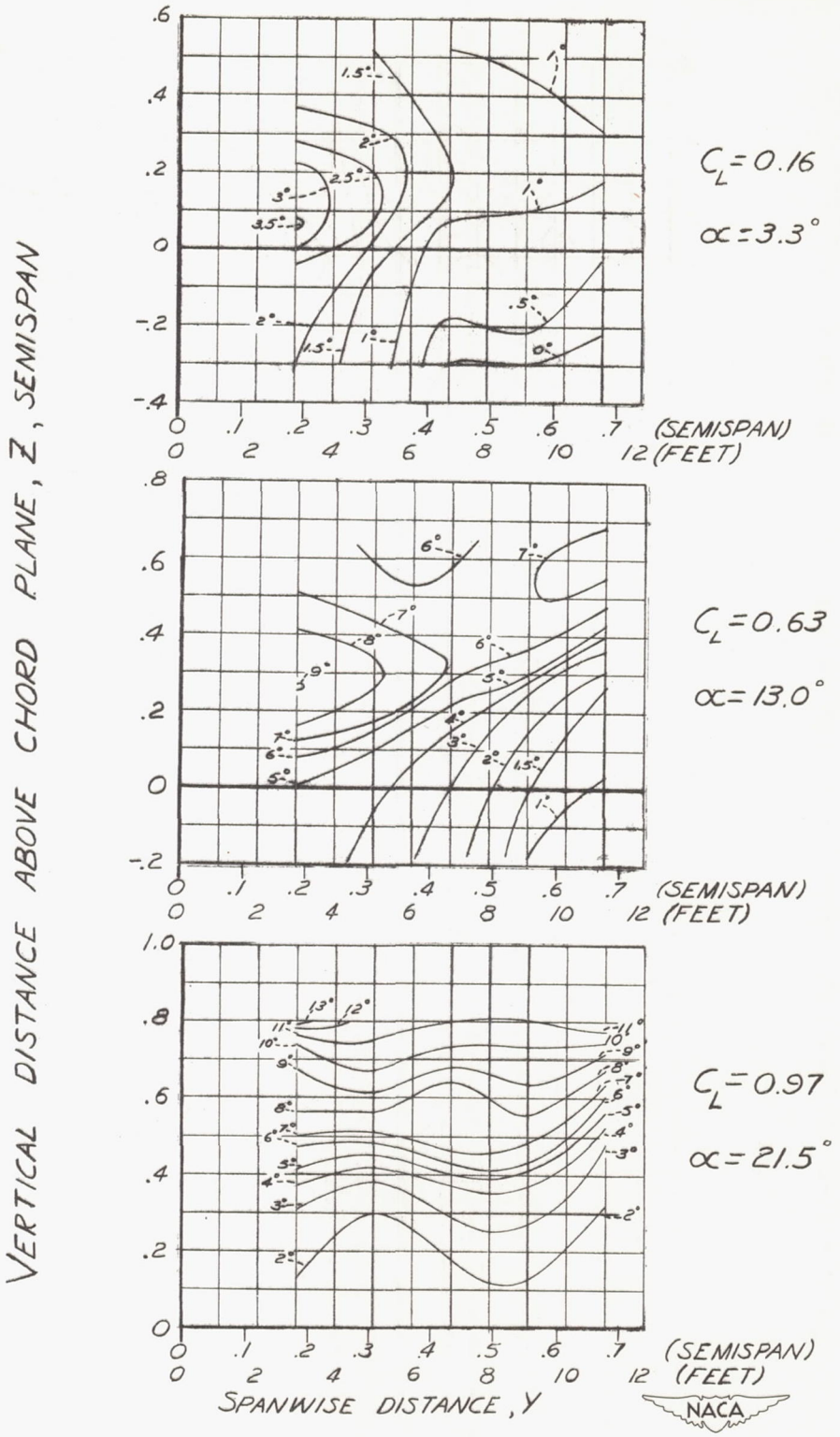


(a) $\Lambda = -45°$

FIGURE 4.— DOWNWASH-ANGLE CONTOURS IN A VERTICAL PLANE 2.8 M.A.C. BEHIND A POINT AT THE .25 M.A.C.

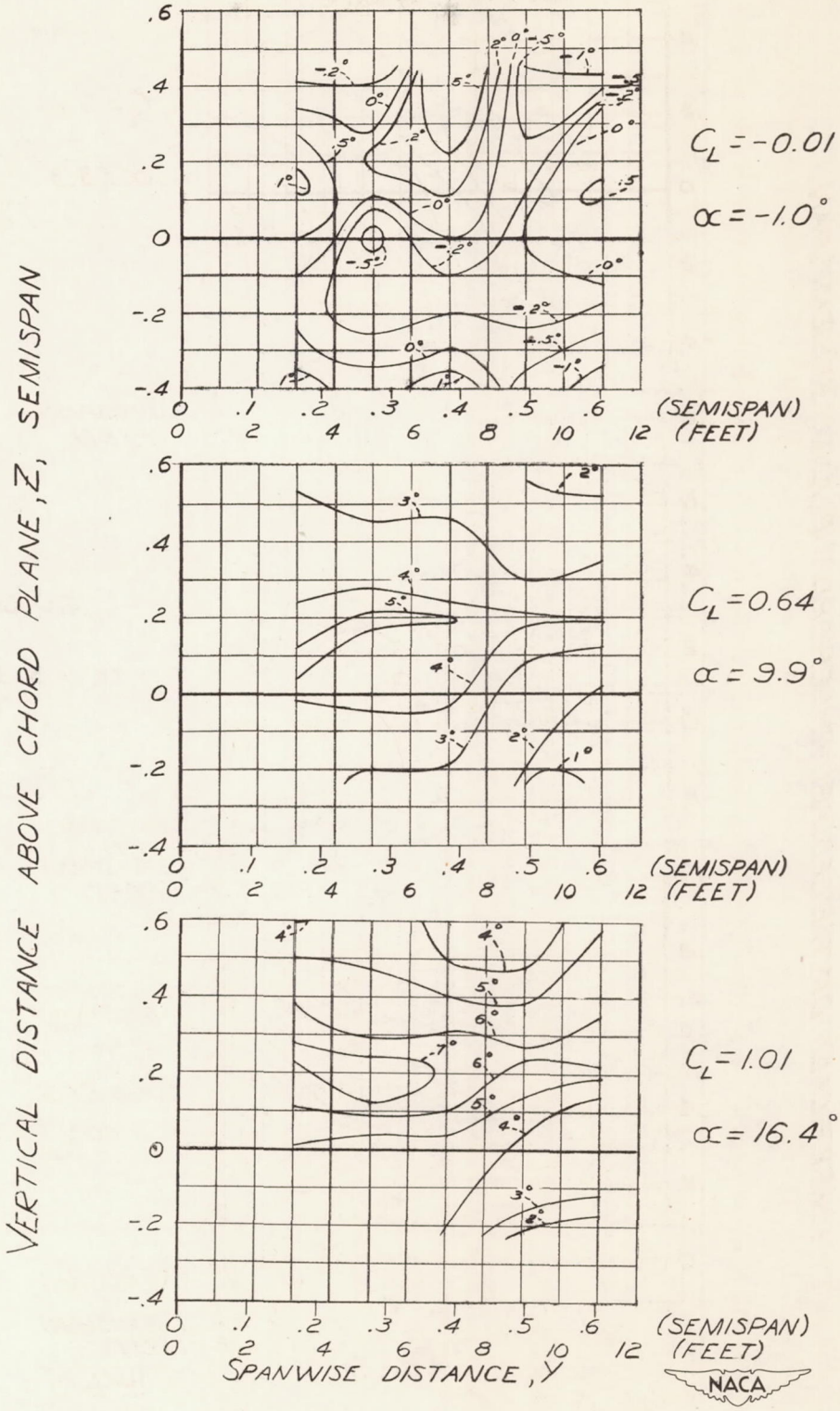


(b) $\Lambda = -30°$

FIGURE 4. — CONTINUED

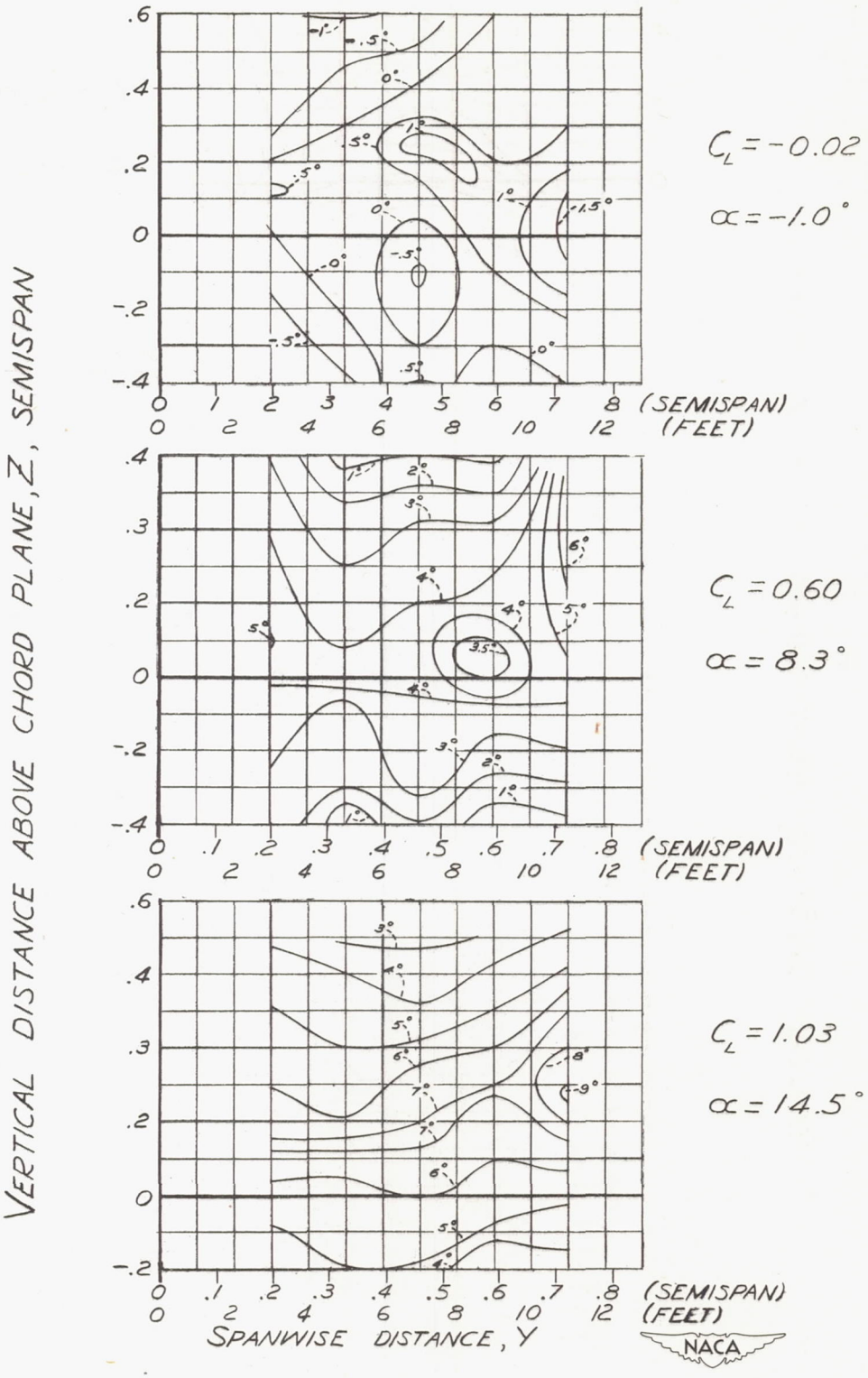


(c) $\Lambda = 0°$

FIGURE 4. — CONTINUED

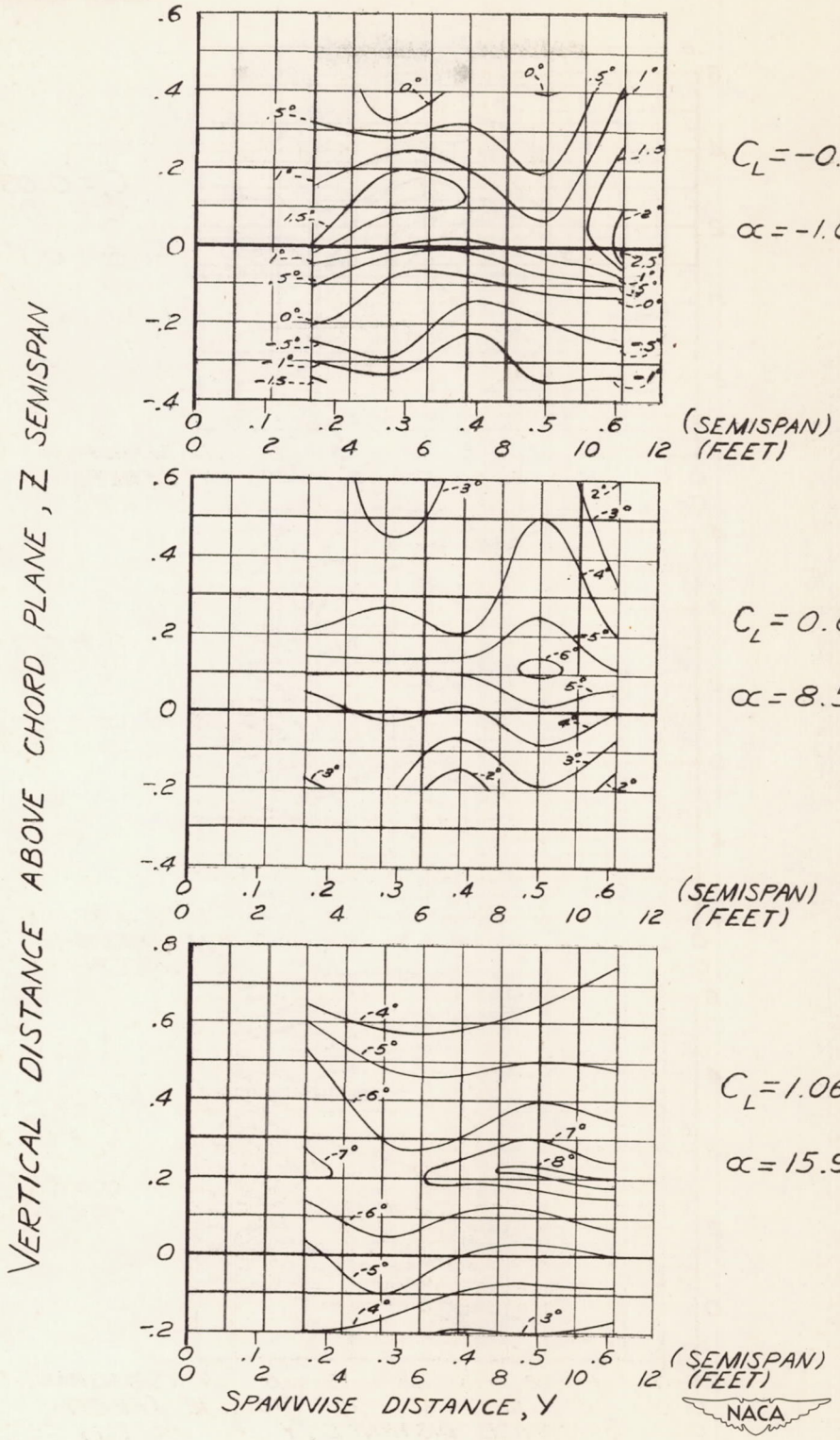


(d) $\Lambda = +30°$

FIGURE 4.— CONTINUED

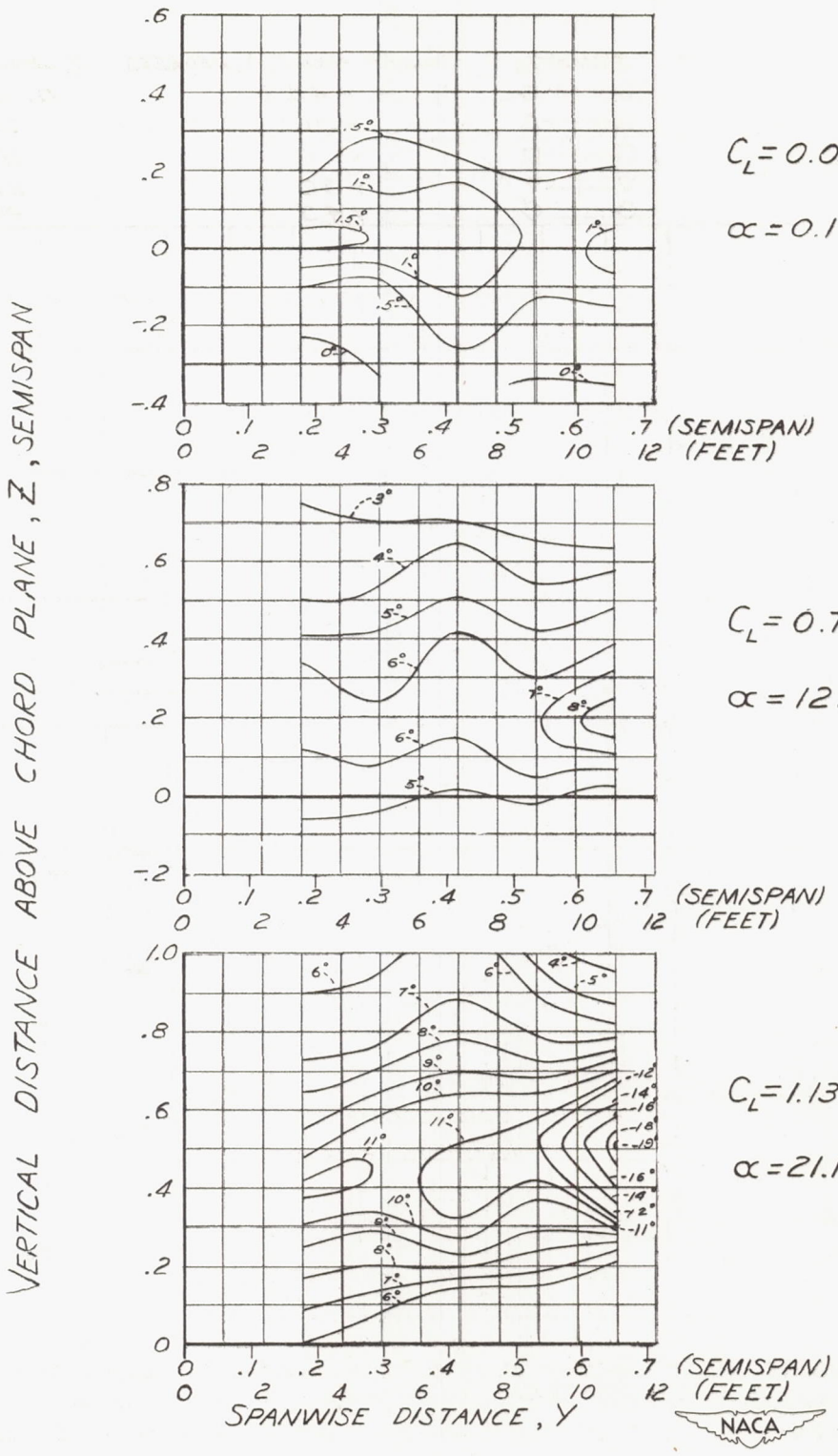


(e) $\Lambda = +45°$

FIGURE 4.— CONCLUDED

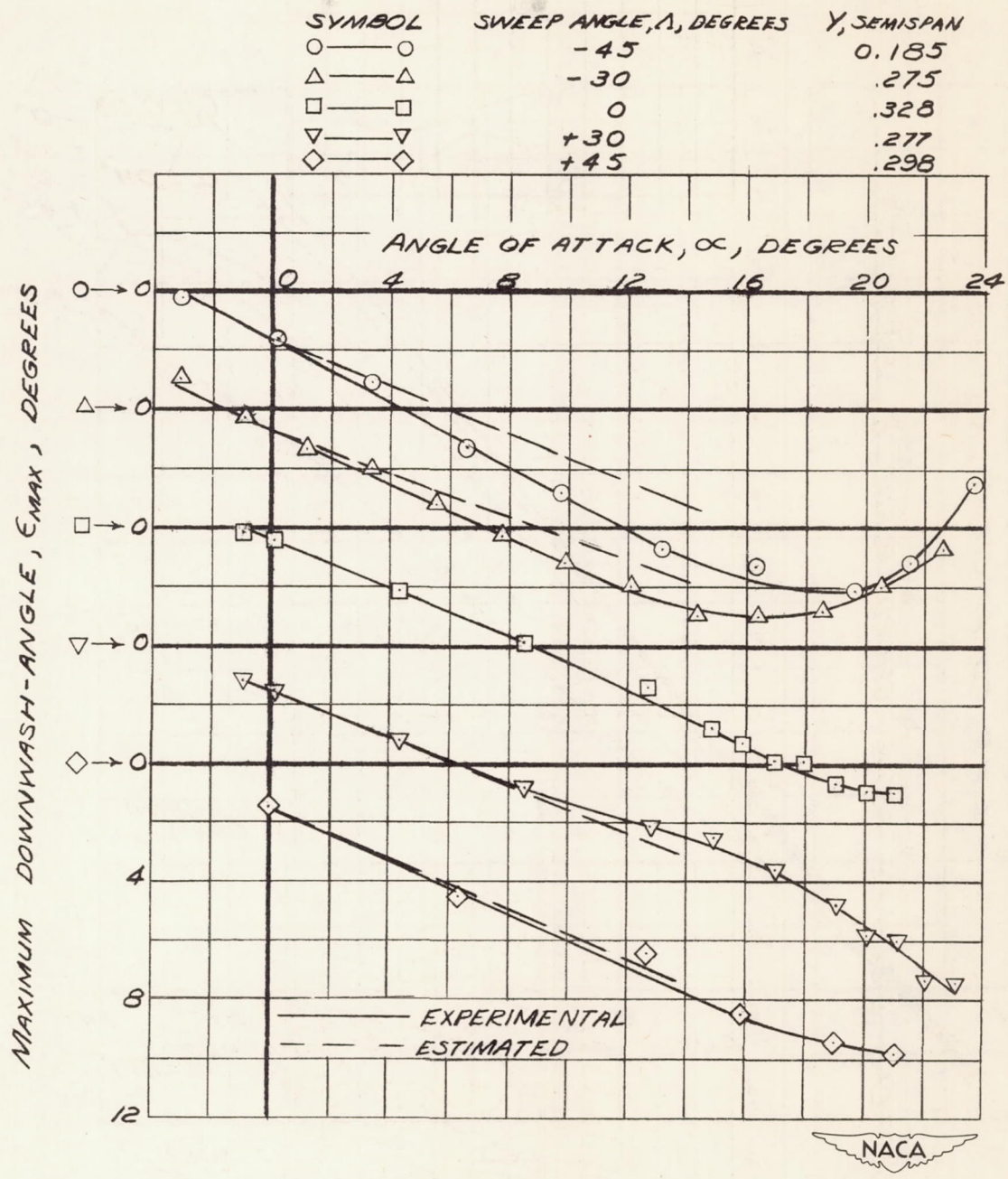


FIGURE 5.—VARIATION OF MAXIMUM DOWNWASH-ANGLE WITH ANGLE OF ATTACK FOR VARIOUS ANGLES OF WING SWEEP AT A POINT 2.8 M.A.C. BEHIND THE .25 M.A.C. POINT.

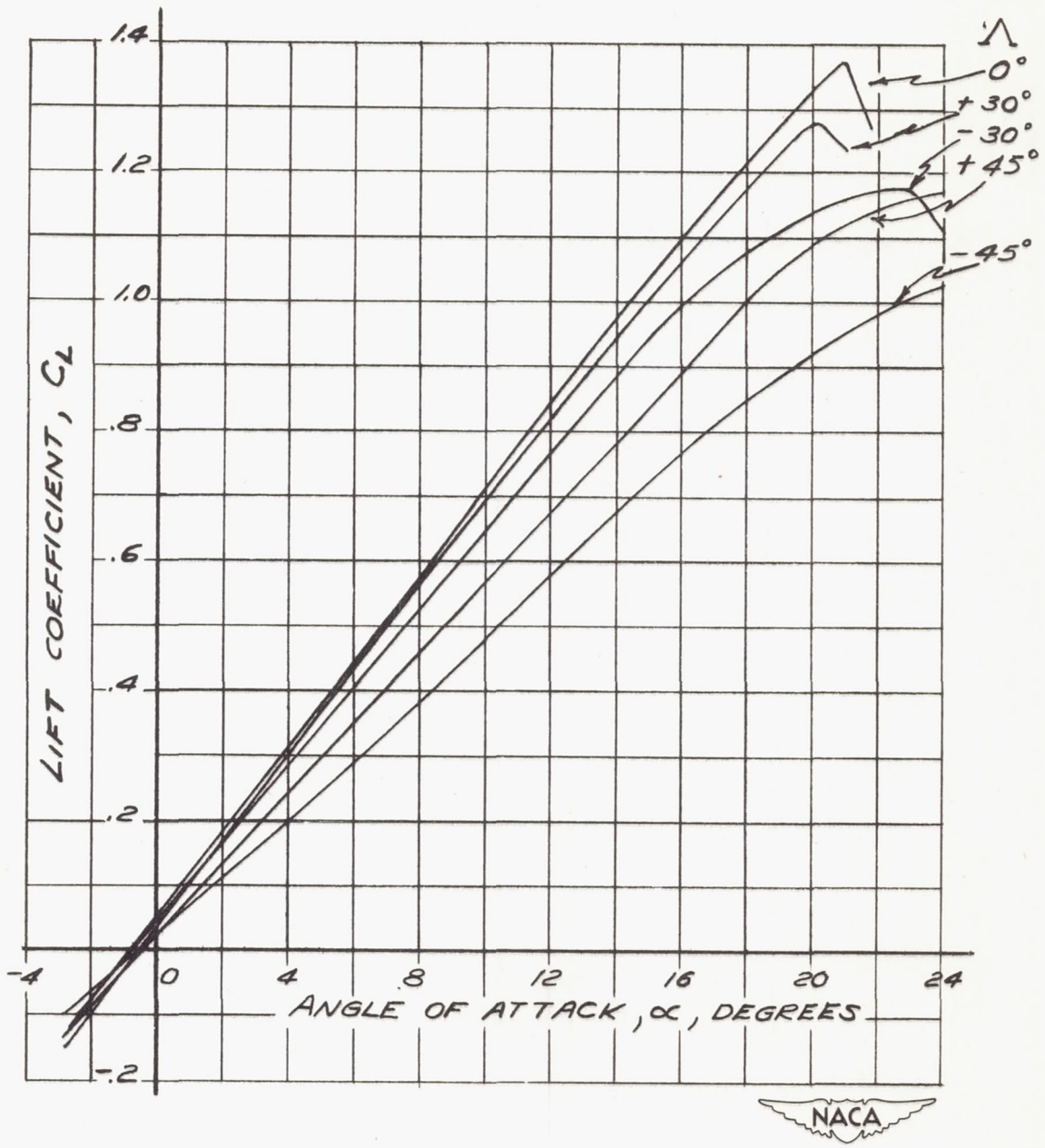


FIGURE 6.— VARIATION OF LIFT COEFFICIENT WITH ANGLE OF ATTACK FOR THE VARIOUS SWEPT WINGS. FROM REFERENCE 1.

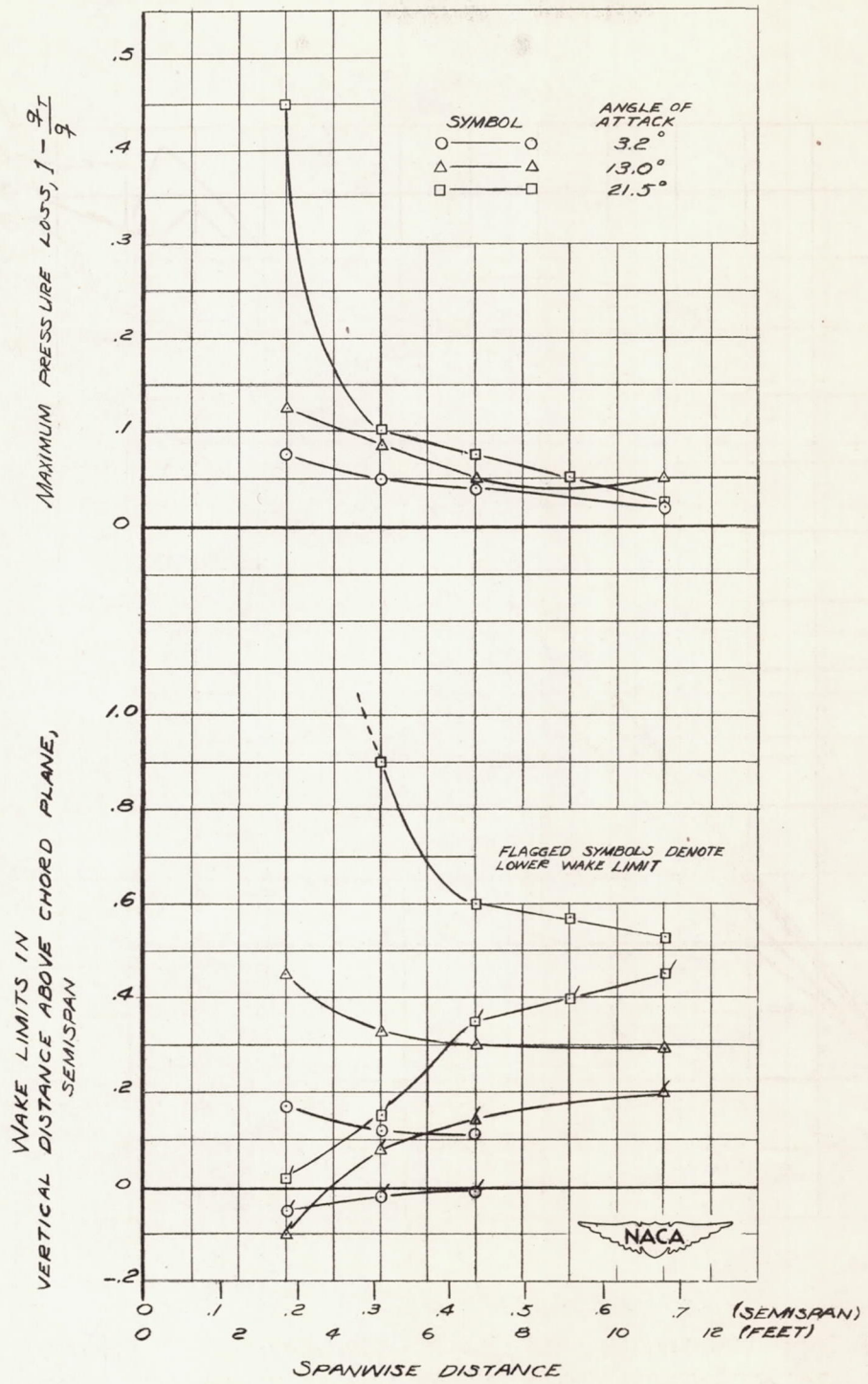


(a) $\Lambda = -45°$

FIGURE 7.— SPANWISE VARIATION OF WAKE LIMITS AND MAXIMUM PRESSURE LOSS IN WAKE IN A VERTICAL TRANSVERSE PLANE 2.8 M.A.C. BEHIND A POINT AT THE .25 M.A.C.

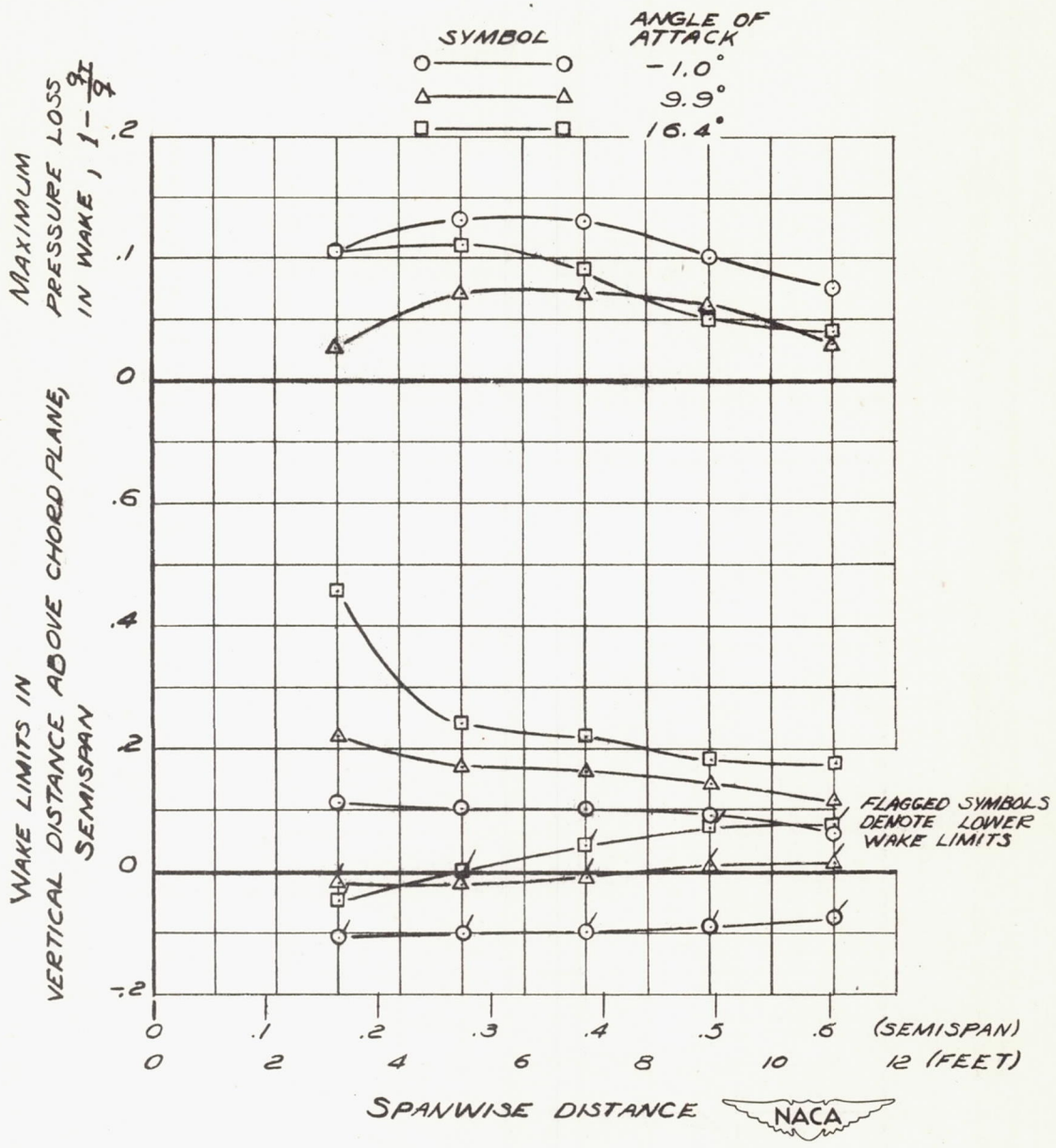


(b) $\Lambda = -30°$

FIGURE 7.— CONTINUED.

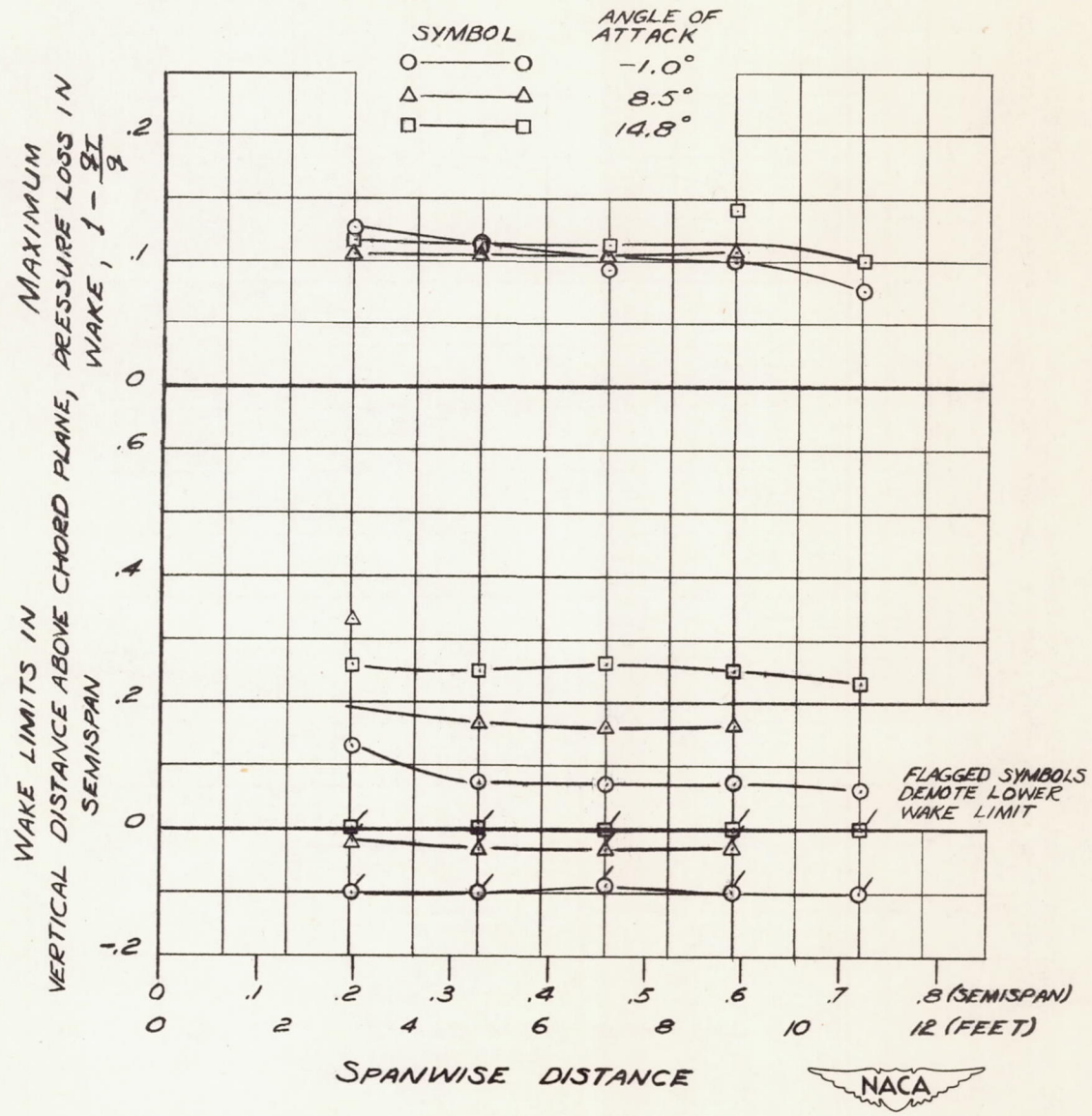


(c) $\Lambda = 0°$

FIGURE 7.- CONTINUED.

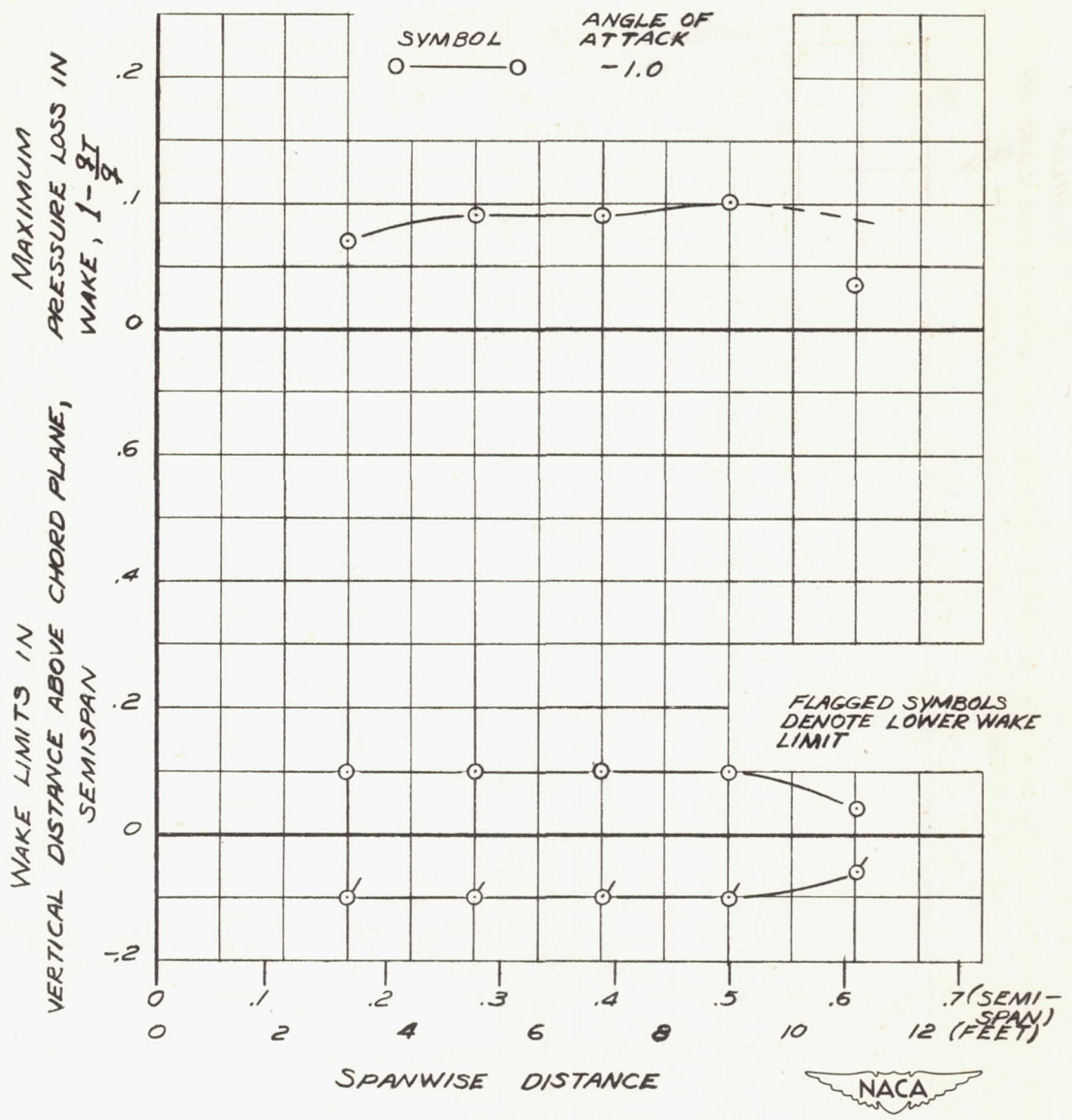


(d) $\Lambda = +30°$

FIGURE 7.- CONTINUED.

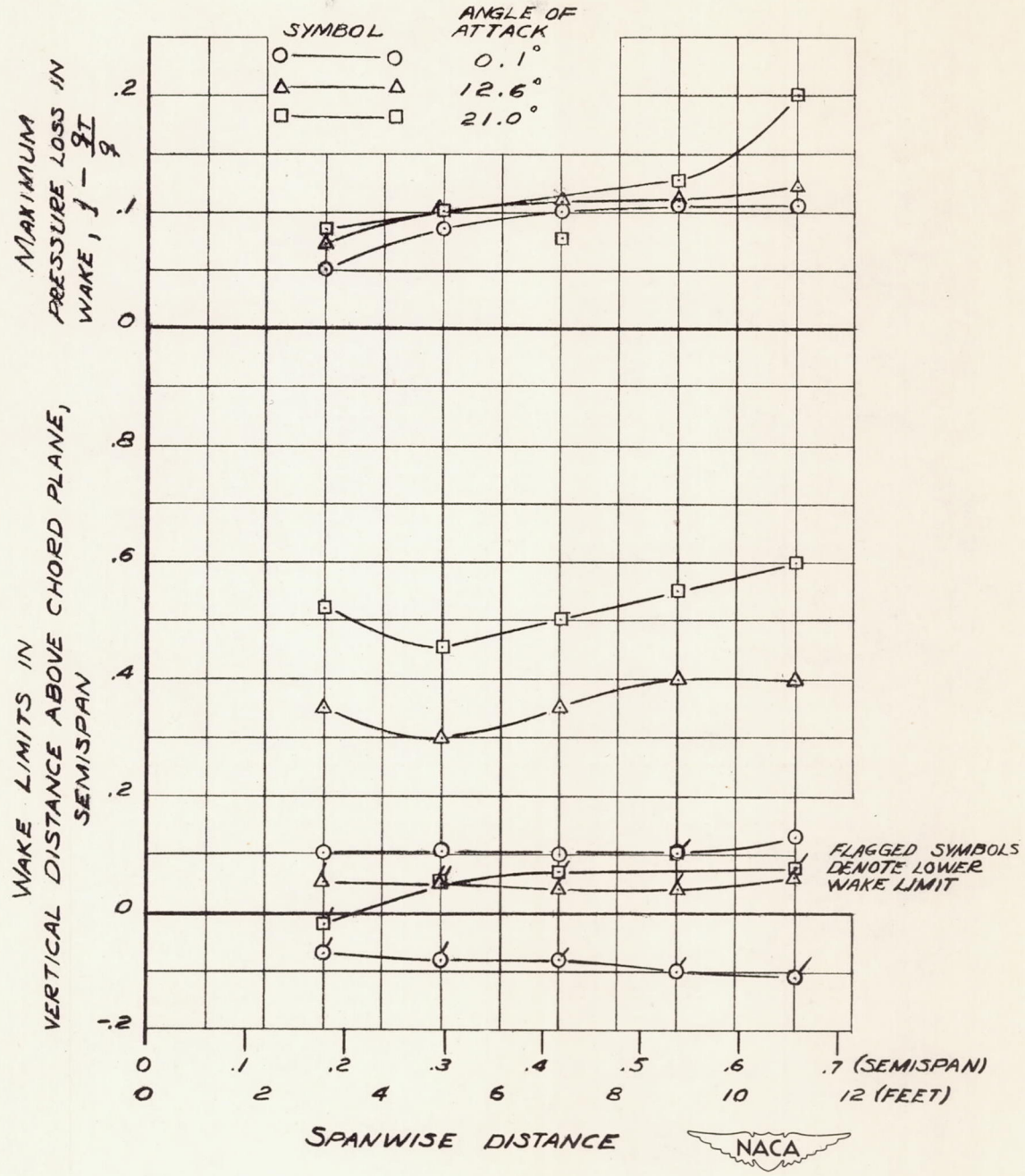


(e) $\Lambda = +45°$

FIGURE 7.— CONCLUDED.